Animal Reproduction Science 282 (2025) 108009

Contents lists available at ScienceDirect

Animal Reproduction Science

journal homepage: www.elsevier.com/locate/anireprosci

Seminal extracellular vesicles influence porcine spermatozoa physiology by modulating key functional parameters

Ana Parra [a,b], Francisco E. Martín-Cano [c], Pablo Martínez-Díaz [a,b], Patricia Panales [a,b], Xiomara Lucas [a,b,*], Jordi Roca [a,b,*], Fernando J. Peña [c], Isabel Barranco [a,b]

[a] Department of Medicine and Animal Surgery, Veterinary Science, University of Murcia, Murcia, Spain
[b] International Excellence Campus for Higher Education and Research "Campus Mare Nostrum", Institute for Biomedical Research of Murcia (IMIB-Arrixaca), University of Murcia, Murcia, Spain
[c] Laboratory of Equine Reproduction and Equine Spermatology, Veterinary Teaching Hospital, University of Extremadura, Cáceres, Spain

ARTICLE INFO

Keywords:
Extracellular vesicles
Seminal plasma
Spermatozoa
Pig
Sperm function

ABSTRACT

Seminal plasma (SP) contains a heterogeneous population of extracellular vesicles (EVs) recognized as key modulators of sperm function. However, the specific functional roles of each seminal EV (sEV) subset remain poorly understood. This study aimed to evaluate the interaction of two sized sEV subsets (small [S-sEVs] and large [L-sEVs]) with pig liquid-stored spermatozoa under different pH conditions and their effect on specific sperm functional parameters. Seminal EV subsets were isolated from SP samples using size exclusion chromatography and characterized following the MISEV2023 guidelines. Semen samples were incubated with each sEV subset or without sEVs (control) for 6 h at 37 ºC, 100 % humidity and 5 % CO_2 under different pH conditions (6.5, 7.0, or 7.5). Sperm functional parameters were assessed by flow cytometry (Cytoflex®S and LX, Beckman Coulter), under capacitating and non-capacitating conditions. Confocal microscopy revealed that both sEV subsets bound to and were internalized by spermatozoa as early as 30 min after incubation, regardless of pH. Flow cytometry revealed that both sEVs decreased reactive oxygen species production ($P \leq 0.0001$), mitochondrial membrane potential ($P \leq 0.0001$) and mitochondrial $O_2^{\bullet-}$ levels ($P \leq 0.01$) and increased apoptosis (active caspase-3) in viable spermatozoa ($P \leq 0.0001$). However, the influence of sEV on acrosome integrity in viable sperm was time- and condition-dependent ($P \leq 0.05$). This study showed that both S- and L-sEVs interact with porcine spermatozoa across a range of physiological pH conditions. This interaction is reflected by decreased oxidative stress and mitochondrial activity, as well as increased apoptosis in spermatozoa.

1. Introduction

Seminal plasma (SP) is a complex fluid that surrounds sperm during and after ejaculation. It is composed of secretions from the male reproductive organs (Rodriguez-Martinez et al., 2021). SP contains a wide range of biomolecules, particularly proteins, which regulate sperm function (Juyena and Stelletta, 2012) and contribute to the immunomodulation of the female reproductive tract, a key

* Corresponding authors at: Department of Medicine and Animal Surgery, Veterinary Science, University of Murcia, Murcia, Spain.
E-mail addresses: xiolucas@um.es (X. Lucas), roca@um.es (J. Roca).

https://doi.org/10.1016/j.anireprosci.2025.108009
Received 18 August 2025; Received in revised form 24 September 2025; Accepted 26 September 2025
Available online 27 September 2025

factor for successful embryo development and implantation (Rodríguez-Martínez et al., 2011). There is increasing evidence showing that some of these active SP biomolecules are loaded into extracellular vesicles (EVs) (Rodriguez-Martinez and Roca, 2022). EVs are nano-sized membrane particles secreted by virtually all functional body cells that play a key role in cell-to-cell communication. They carry cargo rich in bioactive molecules, including nucleic acids, lipids, metabolites and proteins, from donor cells to recipient cells, eliciting specific functional responses (Colombo et al., 2014; Jeppesen et al., 2023). EVs protect their molecular cargo from enzymatic degradation and facilitate their targeted delivery to neighboring or distant cells. Therefore, EVs are involved in many physiological and pathological processes (Doyle and Wang, 2019; Kalluri and LeBleu, 2020), including those affecting the male and female reproductive tracts (Hawke et al., 2021; Machtinger et al., 2021; Mishra et al., 2021; Tamessar et al., 2021).

Seminal EVs (sEVs) have the ability to interact with spermatozoa, which has been demonstrated in several mammalian species (Aalberts et al., 2013; Lange-Consiglio et al., 2022; Murdica et al., 2019), including pigs (Barranco et al., 2024b; Du et al., 2016). This interaction has been linked to changes in sperm function (Roca et al., 2022). However, there is a controversy regarding which sperm parameters are affected and how. Motility is the most commonly analyzed sperm parameter, and studies have reported contradictory results. Most studies have shown that interaction with sEVs improved sperm motility, either increasing the percentage of motile sperm or improving motility quality (Du et al., 2016; Mahdavinezhad et al., 2022; Murdica et al., 2019; Rowlison et al., 2021; Wang et al., 2022). However, other studies concluded that interaction with sEVs had no effect on sperm motility, or even a negative effect (Bechoua et al., 2011; Cordeiro et al., 2021; Tamessar et al., 2024). In addition to more natural causes, such as species or sperm source (epididymis or ejaculate) and storage conditions (fresh, liquid-stored or frozen), discrepancies in results could be attributed to the inherent heterogeneity of the sEV population or to differences in experimental conditions (Roca et al., 2022). EVs circulating in body fluids are known to be heterogeneous in phenotype and composition, regardless of the body fluid (Bordanaba-Florit et al., 2021). The isolation and functional characterization of existing EV subpopulations is a current research topic, and the expected results should provide a better understanding of the biological roles of EVs (Phillips et al., 2021). Regarding experimental conditions, environmental pH affects the interaction between EVs and receptor cells (Nakase et al., 2021). In the case of spermatozoa, studies have shown that environment pH affects not only EV fusion, but also the uptake and transfer of biomolecules, thus influencing the subsequent functional response of spermatozoa (Aalberts et al., 2013; Arienti et al., 1997; Murdica et al., 2019; Tamessar et al., 2024).

With this in mind, the present experimental study aimed to evaluate how two subsets of seminal EVs that differ in size and composition interact and affect the functionality of porcine spermatozoa under different pH environments.

2. Material and methods

2.1. Ethical statement

All experiments performed in this study were approved by the Bioethics Committee of the University of Murcia (research codes CBE-367/2021 and CBE-538/2023) and were conducted in accordance with the Directive 2010/63/EU for the protection of animals used for scientific purposes. Semen samples were obtained from boars included in an artificial insemination (AI) program housed in an AI-center (AIM Iberica, Calasparra, Murcia, Spain) that complies with the Spanish (ES300130640127, August 2006) and European (ES13RS04P, July 2012) regulations regarding the production and commercialization of AI semen doses, as well as animal health and welfare.

2.2. Boars, ejaculates and seminal plasma samples

Entire ejaculates were collected from healthy, sexually mature (two to three years old) boars of different breeds (Pietrain, Landrace and Large White) using a semi-automated procedure (Collectis®, IMV Technologies, L'Aigle, France). All boars were housed in individual pens within a climate-controlled building with a room temperature (RT) range of 15–25 ºC and 16 h of light per day. The boars had unlimited access to water and were fed commercial diets formulated to meet the nutritional requirements of boars in AI-programs.

All ejaculates used in the study met the semen quantity and quality criteria required for producing commercial AI semen doses: a sperm concentration of at least 200 $\times$ 10^6 sperm/mL, motile sperm of at least 70 %, and sperm with normal morphology of at least 75 %.

Immediately after the ejaculate collection, a 10 mL aliquot of each ejaculate was centrifuged at 1500 g twice for 10 min at RT using a Rotofix 32 A centrifuge (Hettich Centrifuge UK, Newport Pagnell, Buckinghamshire, England, UK) for SP collection. To ensure the absence of sperm, the resulting SP was microscopically analyzed (Eclipse E400; Nikon, Tokyo, Japan). To prevent protein degradation, the SP samples were treated with a protease inhibitor cocktail (Complete™ protease inhibitor cocktail tablets; Roche, Basilea, Switzerland). Then, the SP samples were placed in insulated containers and sent to the Animal Andrology research group laboratory at the University of Murcia (Veterinary Teaching Hospital, Campus de Espinardo, Murcia, Spain). Once there, the SP samples were stored at 5 ºC (Zanussi Tropic System, Electrolux España S.A.U, Madrid, Spain) until sEVs isolation.

2.3. Isolation of seminal extracellular vesicles

Seminal EVs were isolated using the size exclusion chromatography (SEC)-based protocol recently published by our research group (Martínez-Díaz et al., 2025). Upon arrival at the laboratory, SP samples (~ 8 mL) were centrifuged at 3200 g for 15 min at 4 ºC using a Sorvall™ ST 40 R centrifuge (Thermo Fisher Scientific, Waltham, Massachusetts, USA) to remove any remaining sperm and cellular *debris*. The supernatants were collected and mixed to generate different pools (see the experimental design section). These pools were

then centrifuged at 20,000 g for 30 min at 4 ºC using a Sorvall™ Legend Micro 21 R centrifuge (Thermo Fisher Scientific). The resulting pellets and supernatants were processed separately. The pellets were diluted in 500 μL of 0.22 μm-filtered (Millex® syringe filters, Merck, Darmstadt, Germany) phosphate-buffered saline (fPBS, Merck) and stored at 5 ºC until SEC. The supernatants were diluted with fPBS (1:2; v:v), filtered with 0.22-μm filters, and ultrafiltered using Amicon® Ultra-4 centrifugal 100-kDa filter devices (Merck) with a 3200 g centrifugation regime for 90 min at 4 ºC. The treated pellets and supernatants were stored at 5 ºC. SEC was performed using Econo-Pac® chromatography columns (Bio-Rad, Hercules, California, USA), which were loaded with 10 mL of Sepharose CL-2B® (Merck). Twenty eluted fractions of 0.5 mL were collected per sample. Large sEVs (L-sEVs) were obtained by mixing the sixth to tenth SEC eluted fractions of pellets samples, and small sEVs (S-sEVs) were obtained by mixing the seventh to eleventh SEC eluted fractions of supernatant samples. Each isolated sEV sample was split into two aliquots. One was diluted (1:1; v:v) with a PBS-HAT solution containing 25 mM HEPES, 25 mM trehalose, and 0.2 % albumin, and stored at −80 ºC for use in sperm functional experiments (see the experimental design section). For use, the isolated sEV samples were thawed on ice, ultrafiltered using Amicon® Ultra-4 centrifugal 100-kDa filter (3200 g 10 minutes) and diluted with appropiated medium.The other was stored at 5 ºC for use in sEV characterization analyses.

2.4. Characterization of seminal extracellular vesicles

To comply with the Minimal information for studies of extracellular vesicles (MISEV 2023) guidelines (Welsh et al., 2024), all sEV samples were characterized using different and complementary techniques. The analyses included the following: (1) measurement of total protein concentration by spectrophotometry, (2) particle size distribution by dynamic light scattering, (3) sEV morphology by transmission electron microscopy, and (4) assessment of EV-specific protein markers, as well as albumin, a non-vesicular extracellular particle, by flow cytometry. The techniques used to characterize the sEV samples are detailed in **Supplementary File S1**.

2.5. Labeling of seminal extracellular vesicles

Both sEV subsets, S-sEVs and L-sEVs, were labeled using Vybrant™ Cell-Labeling Solutions (Thermo Fisher Scientific), according to the protocol described by Murdica et al., (2019). The S-sEVs were stained with Vybrant™ DiI (V22885, Thermo Fisher Scientific; 549 nm excitation, 565 nm emission) and L-sEVs were stained with Vybrant™ DiD (V22887, Thermo Fisher Scientific; 644 nm excitation, 665 nm emission). Briefly, each dye was diluted in fPBS (1:100, v:v) and added to the sEV preparation (1:1, v:v; 0.5 mg/mL) and fPBS (control; 1:1; v:v). The samples were then incubated for 20 min at 37 ºC with gentle agitation (Labnet Orbit P2, Labnet Biotecnica SL, Madrid, Spain). To remove unbound dye, the samples were ultracentrifuged at 150,000 g for 1 h at 4 ºC using an Optima L-100 XP Ultracentrifuge with a SW55 rotor (Beckman Coulter, Brea, California, USA). The resulting pellets containing the stained sEVs were split into three aliquots and resuspended with Tyrode medium (T2145, Merck; 200 μL) at three different pHs: 6.5, 7 and 7.5. The stained sEV samples were stored at 5 ºC until use in Experiment 1 (see the experimental design section).

2.6. Assessment of sperm functional parameters using flow cytometry

Sperm functional parameters were assessed using Cytoflex S® and Cytoflex LX® flow cytometers (Beckman Coulter), following the protocols described by Becerro-Rey et al., (2024), which were adapted for pig spermatozoa. The Cytoflex S® was equipped with lasers emitting at 405 nm (violet), 488 nm (blue), 561 nm (yellow), and 638 nm (red), while the Cytoflex LX® was equipped with lasers emitting at 355 nm (ultraviolet), 405 nm (violet), 488 nm (blue), 561 nm (yellow), 638 nm (red) and 808 nm (infrared). Both instruments underwent daily calibration using commercially available calibration beads. The data were exported as FCS files, analyzed and compensated using FlowJo™ V10.8.1 (Ashland, OR, USA) and Cytobank™ (Beckman Coulter; https://premium.cytobank.org/cytobank/login) software. According to the Minimum Information About a Flow Cytometry Experiment (MIFlowCyt) standard guidelines (Lee et al., 2008), unstained and single-stained semen samples, as well as fluorescence minus one control, were used to establish compensation, identify positive and negative events, and define regions of analysis. A total of 30,000 spermatozoa were analyzed per semen sample.

The functionality of viable sperm was assessed in terms of acrosome membrane integrity, mitochondrial $O_2^{\bullet-}$ production, intracellular Ca^{2+}, mitochondrial membrane potential (MMP), apoptosis (active caspase-3) and total reactive oxygen species (ROS) production.

2.6.1. Assessment of sperm acrosome membrane integrity, mitochondrial $O_2^{\bullet-}$ production, and intracellular Ca^{2+}

A four-color panel was developed on the CytoFLEX LX® to evaluate multiple sperm functionality parameters simultaneously. Specifically, it evaluates viability, mitochondrial $O_2^{\bullet-}$ production, acrosome membrane integrity and intracellular Ca^{2+}. Briefly, sperm samples (100 μL; 1×10^6 spermatozoa) were diluted with 400 μL of PBS and stained with (1) 2 μL of ViaKrome 808 (C36628, Beckman Coulter; excitation/emission: 854/878 nm) to assess viability; (2) 1 μL of a 0.25 mg/mL solution of PNA-Alexa Fluor 647 Conjugate (L32460, Thermo Fisher Scientific; excitation/emission: 650/668 nm) to assess acrosome membrane integrity; (3) 0.5 μL of a 5 mM solution of MitoSOX Red (M36007, Thermo Fisher Scientific; excitation/emission: 396/610 nm) to measure mitochondrial $O_2^{\bullet-}$ production; and (4) 1 μL of a 50 μM solution of Fluo4 (F14201, Thermo Fisher Scientific; excitation/emission: 494/506 nm) to assess intracellular Ca^{2+}. The samples were incubated at 37 ºC for 20 min in the dark, washed by centrifugation, and diluted to 500 μL of PBS before analysis.

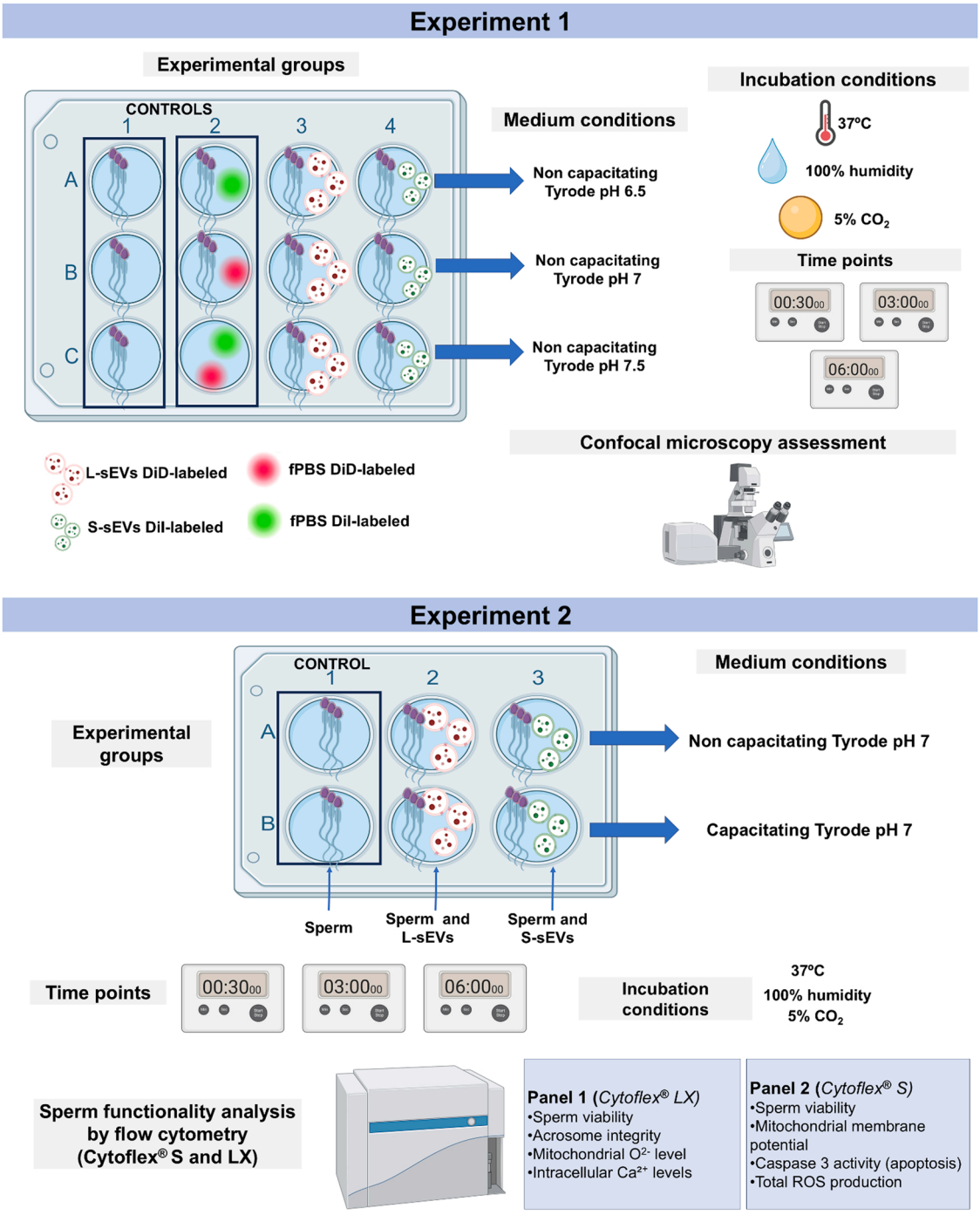

Fig. 1. Experimental design. *Experiment 1*: Analysis of the interaction between small (S) and large (L) seminal extracellular vesicle (sEV) subsets and porcine liquid-stored spermatozoa under three pH conditions (6.5, 7.0, and 7.5). Spermatozoa were incubated with DiI-labeled S-sEVs or DiD-labeled L-sEVs for six hours and analyzed at three time points (30 min, 3 h, and 6 h) by confocal microscopy. Controls included sperm samples without sEVs and with either DiI- or DiD-labeled filtered Phosphate Buffer Saline (fPBS) or both DiI- and DiD-labeled fPBS, but without sperm. Three biological replicates were performed. *Experiment 2*: Assessment of the effects of sEV subsets on sperm functionality parameters conditions. Spermatozoa were incubated with S-sEVs or L-sEVs, under capacitating and non-capacitating, for six hours and analyzed at three time points (30 min, 3 h, and 6 h) by flow cytometry. Four biological replicates were performed. ROS: reactive oxygen species. Created using *Biorender.com*.

2.6.2. Assessment of MMP, apoptosis and total ROS production

A multiparametric panel was created on the Cytoflex S® to assess multiple sperm functionality parameters simultaneously. Specifically, it evaluates viability, MMP, total ROS production and apoptosis. Briefly, 100 μL aliquot of each sperm sample (1×10^6 spermatozoa) was diluted with 400 μL of PBS and stained with (1) 1 μL of LIVE/DEAD Fixable Violet Dead Cell Stain Kit (L34957, Thermo Fisher Scientific; excitation/emission: 405/450 nm) to determine viability; (2) 0.5 μL of a 100 μM solution of tetramethylrhodamine (I3436, Thermo Fisher Scientific; excitation/emission: 548/574 nm) to assess MMP, (3) 0.5 μL of a 2 mM solution of CellEvent™ Caspase-3/7 Green Detection (C10423, Thermo Fisher Scientific; excitation/emission: 502/530 nm) to detect apoptosis; and (4) 0.5 μL of a 2.5 mM solution of CellRox deep red (C10422, Thermo Fisher Scientific; excitation/emission: 638/665 nm) to measure total ROS production ($O_2^{\bullet -}$ and hydroxyl radicals). The samples were incubated at 37 ºC for 20 min in the dark, washed by centrifugation, and diluted to 500 μL of PBS before analysis.

2.7. Experimental design

Fig. 1 illustrates a schematic overview of the experimental design of the study.

2.7.1. Experiment 1: Interaction of sEV subsets with liquid-stored spermatozoa under different pH conditions

Commercial liquid-stored semen AI doses (30×10^6 spermatozoa/mL) from 12 boars were randomly mixed into three separate pools, each containing samples from four boars. The semen pools were centrifuged at 2300 g for 3 min at 17 ºC using a Sorvall™ ST 40 R centrifuge (Thermo Fisher Scientific). The resulting sperm pellets were divided into three aliquots and resuspended in Tyrode medium adjusted at pH levels of 6.5, 7, and 7.5 until the final concentration reached 50×10^6 spermatozoa/mL. Then, 40 μL of each sperm sample was diluted in 360 μL of Tyrode medium (5×10^6 spermatozoa/mL) containing either DiI-labeled S-sEVs (0.5 mg/mL) or DiD-labeled L-sEVs (0.5 mg/mL). The samples were incubated for up to 6 h at 37 ºC with 5 % CO_2, and 100 % humidity, while being shaken in the dark (Labnet Orbit P2). Four control sperm samples diluted in Tyrode medium were included: (1) without sEVs, (2) with DiD-labeled fPBS, (3) with DiI-labeled fPBS; and (4) without sperm and DiI- and DiD-labeled fPBS.

At three different time points (30 min, 3 and 6 h), 100-μL aliquot of each sample were centrifuged at 3000 g for 20 min at RT using a Sorvall™ Legend Micro 21 R centrifuge to remove free circulating sEVs. The resulting sperm pellets were resuspended in 20 μL of Tyrode medium. The samples were then incubated for 10 min at 37 °C with 2 μL of a 0.05 mg/mL solution of Hoechst 33342 (B2261, Merck), fixed with 4 % paraformaldehyde (1:1; CAS 30525–89–4, Merck), and mixed with a VECTASHIELD Antifade (Newark, California, USA). The samples were then mounted on slides, coverslipped, and examined using a Stellaris 8 confocal microscope (Leica Microsystems S.L.U, Wetzlar, Germany), which was equipped with a white light laser and a 63X/1.30 NA glycerol immersion objective (506353, Leica Microsystems), in order to assess the binding and uptake of sEVs in the spermatozoa.

2.7.2. Experiment 2: Effect of sEV subsets on sperm functional parameters

Commercial liquid-stored semen AI doses (30×10^6 spermatozoa/mL) from 16 boars were randomly mixed into four separate pools, with each pool containing semen samples from four boars. The semen pools were then centrifuged at 2300 g for 3 min at 17 ºC using a Sorvall™ ST 40 R centrifuge. The resulting sperm pellets were divided into two aliquots and resuspended at 20×10^6 spermatozoa/mL in either capacitating (with $NaHCO_3$) or non-capacitating (without $NaHCO_3$) Tyrode medium at pH 7. Then, 175 μL of each sperm sample was diluted in 175 μL of capacitating or non-capacitating Tyrode medium containing either S-sEVs (1 mg/mL), L-sEVs (1 mg/mL) or no sEVs (control). The samples were incubated for 6 h under the same conditions described in Experiment 1. Sperm functional parameters were assessed by flow cytometry at three different time points: 30 min, 3 h and 6 h.

2.8. Statistical analysis

Statistical analyses were conducted using GraphPad Prism 10.5.0 (GraphPad Software, Inc., La Jolla, CA, USA; https://www.graphpad.com/). First, the Shapiro-Wilk test was used to evaluate the normality of the data distribution. Next, a two-way ANOVA analysis was performed to evaluate the potential influence of sEVs (L-sEVs and S-sEVs) and time points (30 min, 3 h, 6 h) on sperm functionality parameters. For multiple comparisons, the Tukey test was applied. Differences were considered statistically significant at $P \leq 0.05$.

3. Results

3.1. Characterization of sEV subsets

Characterization analyses of the sEV samples revealed a highly pure sEV population in all of them. These analyses also confirmed differences in size distribution between S- and L-sEV subsets. Detailed characterization data are provided in Supplementary File S2.

3.2. Interaction of sEV subsets with liquid-stored spermatozoa

Confocal microscopy imaging revealed that both S- and L-sEV subsets interacted with liquid-stored spermatozoa by binding to the head, midpiece, and tail regions, regardless of the pH of the medium (Supplementary Fig. S1). Three-dimensional visualization of this interaction revealed that S- and L-sEVs can bind to and be internalized by spermatozoa as early as 30 min post-incubation, regardless of

the pH of the medium (Fig. 2). Controls confirmed the absence of red/green fluorescence, ruling out any non-specific labeling (Supplementary Fig. S2). Since both sEV subsets interacted with liquid-stored spermatozoa under the three pH conditions, we selected medium at pH 7 for subsequent sperm functional experiment.

3.3. Effect of sEV subsets on sperm functionality parameters

Sperm functionality was evaluated in terms of total ROS production, MMP, mitochondrial $O_2^{\bullet-}$ production, apoptosis (active caspase-3), Ca^{+2} concentration, and acrosome integrity at three different time points (30 min, 3 and 6 h) in sperm samples incubated under capacitating and non-capacitating conditions. The results are expressed relative to viable sperm, the percentage of which is summarized in Supplementary Table S1.

3.3.1. Total ROS production

Under non-capacitating conditions, the percentage of viable sperm with high ROS production differed among treatments ($P \leq 0.0001$) but not among time points (Fig. 3**A**). The percentage of viable sperm with high ROS production was higher in control than in the sEV treatments, and there were no differences between the two sEV subsets. Under capacitating conditions, the percentage of viable sperm with high ROS production differed among treatments ($P \leq 0.0001$) and among time points ($P \leq 0.0001$). There was an interaction ($P \leq 0.0001$) between the two variables (Fig. 3**B**). The pattern was consistent with that observed under non-capacitating conditions; there was higher ROS production in the control than in the sEV treatments at all evaluation time points. The sperm populations identified in the flow cytometry analysis are shown in Supplementary Fig. S3.

3.3.2. Mitochondrial membrane potential

Under non-capacitating conditions, the percentage of viable sperm with high MMP differed among the treatments ($P \leq 0.0001$), but not among the time points. There was an interaction ($P \leq 0.0001$) between the two variables (Fig. 4**A**). The control had a higher percentage of viable sperm with high MMP than in the sEV treatments, and there were no differences between the two sEV subsets. Under capacitating conditions, the percentage of viable sperm with high MMP differed among treatments ($P \leq 0.0001$) and among time points ($P \leq 0.01$). There was an interaction ($P \leq 0.0001$) between the two variables (Fig. 4**B**). After 3 and 6 h of incubation, the percentage of viable sperm with high MMP was higher in control than in the sEV treatments. There were no differences between the two sEV subsets. The sperm populations identified in the flow cytometry analysis are shown in Supplementary Fig. S3.

3.3.3. Mitochondrial $O_2^{\bullet-}$ production

Under non-capacitating conditions, the percentage of viable sperm with mitochondrial $O_2^{\bullet-}$ production (estimated as Relative Fluorescence Units [RFU]) differed among the treatments ($P \leq 0.01$) and among the time points ($P \leq 0.0001$) (Fig. 5**A**). After 30 min of incubation, the control had a higher mitochondrial $O_2^{\bullet-}$ production than the sEV treatments, and there were no differences between the two sEV subsets. Under capacitating conditions, the percentage of viable sperm with mitochondrial $O_2^{\bullet-}$ production differed among the treatments ($P \leq 0.05$) and among the time points ($P \leq 0.0001$). There was an interaction between the two variables ($P \leq 0.0001$) (Fig. 5**B**). After 30 min of incubation the control had a higher mitochondrial $O_2^{\bullet-}$ production than the sEV treatments. However, after 3 and 6 h of incubation, the L-sEV treatment showed higher mitochondrial $O_2^{\bullet-}$ production than the control. The sperm populations identified in the flow cytometry analysis are shown in Supplementary Fig. S3.

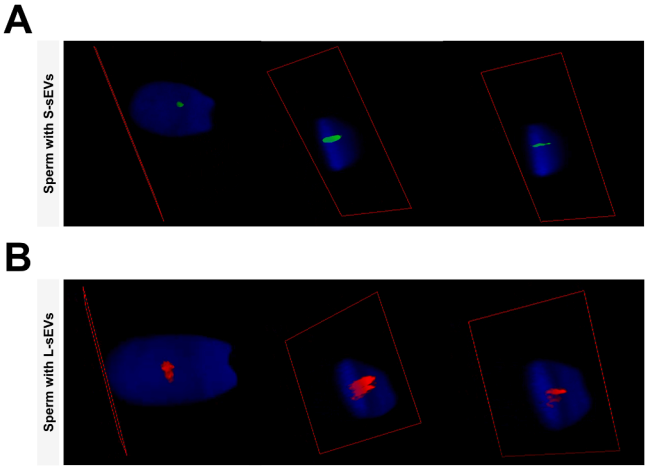

Fig. 2. Representative three-dimensional confocal microscopy images showing the binding and internalization of small (S) and large (L) seminal extracellular vesicles (sEVs) in liquid-stored porcine spermatozoa after 30 min of incubation at 37 °C, 5 % CO_2 and 100 % humidity. The spermatozoa were stained with Hoechst 33342 (blue) and (**A**) S-sEVs with DiI (green), and (**B**) L-sEVs, with DiD (red). Three biological replicates were conducted.

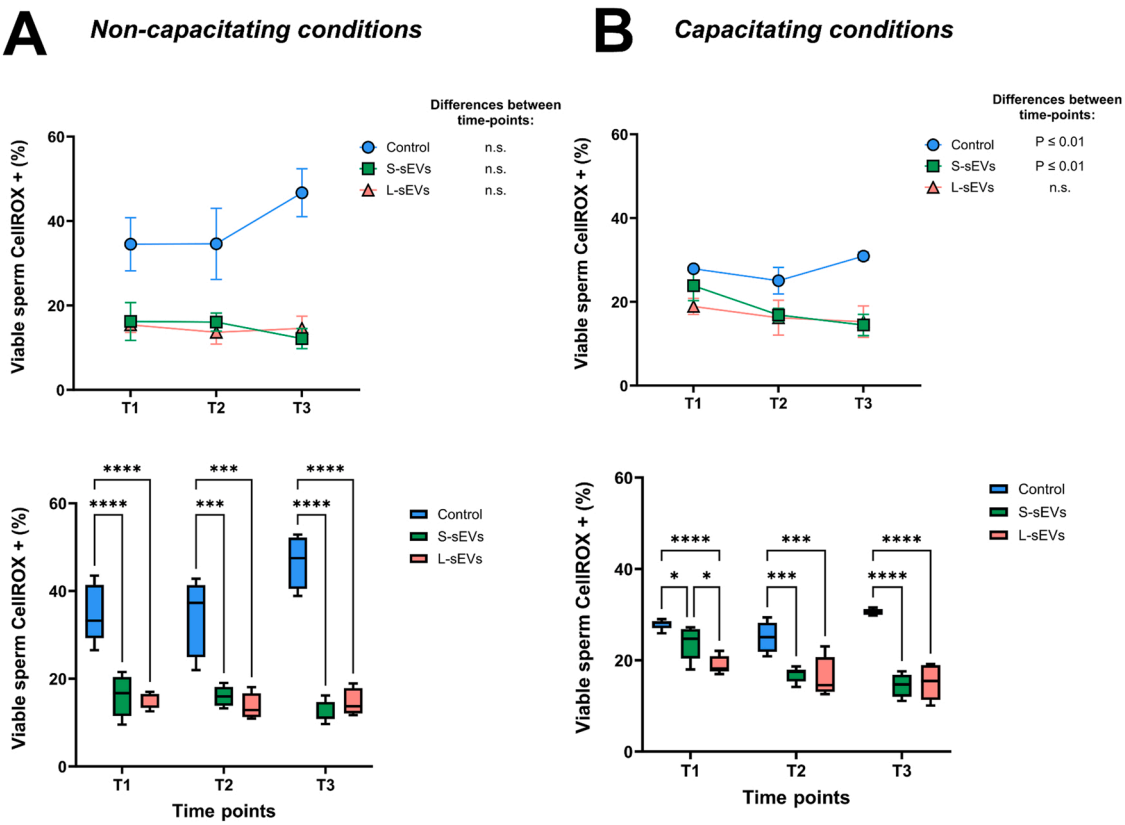

Fig. 3. Percentage of viable spermatozoa with high reactive oxygen species (CellROX+) in porcine liquid-stored sperm samples incubated with small (S-, green), large (L-, red), or no (control, blue) seminal extracellular vesicles (sEVs) under (**A**) non-capacitating and (**B**) capacitating conditions. Data are shown at three time points during incubation at 37 ºC, 5 % CO_2 and 100 % humidity: 30 min (T1), 3 h (T2), and 6 h (T3). The upper graphs show the mean ± SEM, and the lower graphs show box plots (boxes enclose the 25th and 75th percentiles; whiskers extend to the 5th and 95th percentiles; and the line represents the median). Four biological replicates were performed. Differences between time points within each treatment are indicated on the right side of the upper graph. Differences between treatments are shown in the lower graphs. * $P \leq 0.05$, *** $P \leq 0.001$, **** $P \leq 0.0001$, and n.s.: no significant.

3.3.4. *Apoptosis*

Under both non-capacitating and capacitating conditions, the percentage of viable sperm undergoing apoptosis (active caspase-3) varied among the treatments ($P \leq 0.0001$) and among the time points ($P \leq 0.0001$). There was interaction between treatment × time points ($P \leq 0.05$) (Fig. 6). At all-time points, the control had a lower percentage of apoptotic sperm than the sEV treatments, and this pattern was consistent in both non-capacitating and capacitating conditions. The sperm populations identified in the flow cytometry analysis are shown in Supplementary Fig. S3.

3.3.5. *Ca^{+2} concentration*

Under both non-capacitating and capacitating conditions, the intracellular Ca^{+2} concentration in viable sperm (expressed as RFU) differed among the time points ($P \leq 0.01$), but not among treatments (Fig. 7). In both conditions, Ca^{+2} concentration increased after 3 h of incubation in all treatments. The sperm populations identified in the flow cytometry analysis are shown in Supplementary Fig. S3.

3.3.6. *Acrosome integrity*

Under non-capacitating conditions, the percentage of viable acrosome-reacted sperm differed among treatments ($P \leq 0.05$) and among the time points ($P \leq 0.0001$). There was an interaction ($P \leq 0.0001$) between the two variables (Fig. 8**A**). The percentage of viable acrosome-reacted sperm was lower in the control than in the sEV treatments after 30 min of incubation, but higher after 3 h of incubation compared to S-sEV treatment. At 6 h of incubation, this percentage was higher in control than in the S-sEV treatment, with no differences between the S- and L-sEV treatments. Under capacitating conditions, the percentage of viable acrosome-reacted sperm differed among time points ($P \leq 0.0001$), but not among treatments. There was an interaction between the two variables ($P \leq 0.0001$) (Fig. 8**B**). The sperm populations identified in the flow cytometry analysis are shown in Supplementary Fig. S3.

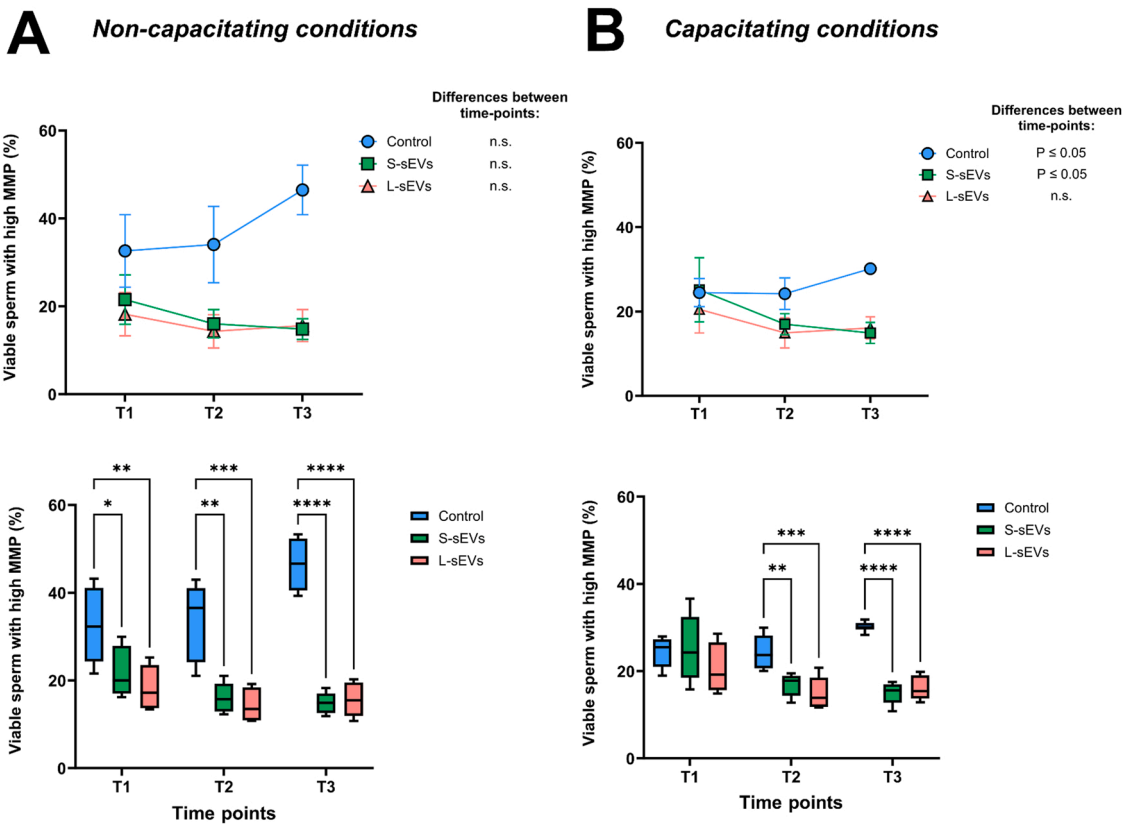

Fig. 4. Percentage of viable sperm with high mitochondrial membrane potential (MMP) in porcine liquid-stored sperm samples incubated with small (S-, green), large (L-, red), or no (control, blue) seminal extracellular vesicles (sEVs) under (**A**) non-capacitating and (**B**) capacitating conditions. Data are shown at three different time points during incubation at 37 °C, 5 % CO_2 and 100 % humidity: 30 min (T1), 3 h (T2), and 6 h (T3). The upper graphs show the mean ± SEM and the lower graphs show box plots (boxes enclose the 25th and 75th percentiles, whiskers extend to the 5th and 95th percentiles, and the line represents the median). Four biological replicates were performed. Differences between time points within each treatment are indicated on the right side of the upper graphs. Differences between treatments are shown in the lower graphs. * $P \leq 0.05$, ** $P \leq 0.01$, *** $P \leq 0.001$, **** $P \leq 0.0001$, and n.s.: no significant.

4. Discussion

This study demonstrated that both S- and L-sEVs can interact with liquid-stored porcine spermatozoa over a wide range of physiological pH values. Furthermore, both sEV subsets modulated key functional sperm parameters, including total ROS and mitochondrial $O_2^{\bullet-}$ production, MMP, apoptosis, and acrosome reaction under both capacitating and non-capacitating conditions.

The biological importance of EVs lies in their ability to interact with target cells, to which they deliver their contents to trigger functional responses (Colombo et al., 2014). Microenvironmental factors, such as pH, can influence the interaction between EVs and target cells (Nakase et al., 2021; Parolini et al., 2009). Several studies have demonstrated that sperm-sEV interaction is pH-dependent (Aalberts et al., 2013; Arienti et al., 1997; Murdica et al., 2019; Pal et al., 2025; Schwarz et al., 2013; Tamessar et al., 2024). This may be associated with the different pH environments of the female reproductive tract through which spermatozoa travel (Park et al., 2011). However, the optimal pH conditions for sEV-sperm binding and fusion are still debated. For instance, Aalberts et al., (2013) reported that the optimal pH for binding sEVs to viable equine sperm was neutral or slightly alkaline. Pal et al., (2025) reached similar conclusions in bovine, reporting that the sEV uptake by spermatozoa was higher at pH 6.8. In contrast, studies in humans have reported that sEV-sperm fusion occurs in a slightly acidic environment (Arienti et al., 1997; Murdica et al., 2019). In our study, confocal microscopy imaging showed that both sEV subsets successfully bound and fused with porcine spermatozoa at three evaluated pH conditions: 6.5, 7.0, and 7.5. Binding of both sEV subsets was evident in the head, midpiece, and tail regions of spermatozoa as early as 30 min after incubation. These results are consistent with those reported by Tamessar et al., (2024), who observed no influence of pH (5.0 *vs.* 7.0) on the interaction between sEVs and human spermatozoa, or on the regions of spermatozoa to which sEVs bind. However, Aalberts et al., (2013) found that the sEV binding to viable equine sperm was restricted to the head in neutral or slightly alkaline conditions. The discrepancies in the influence of environmental pH on sEV-sperm binding patterns may be related to species-specific reproductive differences, including environmental differences in the female reproductive tract. Additionally, the different binding sites may reflect the specific functional roles of sEVs. For instance, given that the midpiece contains mitochondria, sEV binding in this region could regulate the metabolic activity necessary for motility (Tamessar et al., 2024). In view of the absence of differences in sEV-sperm

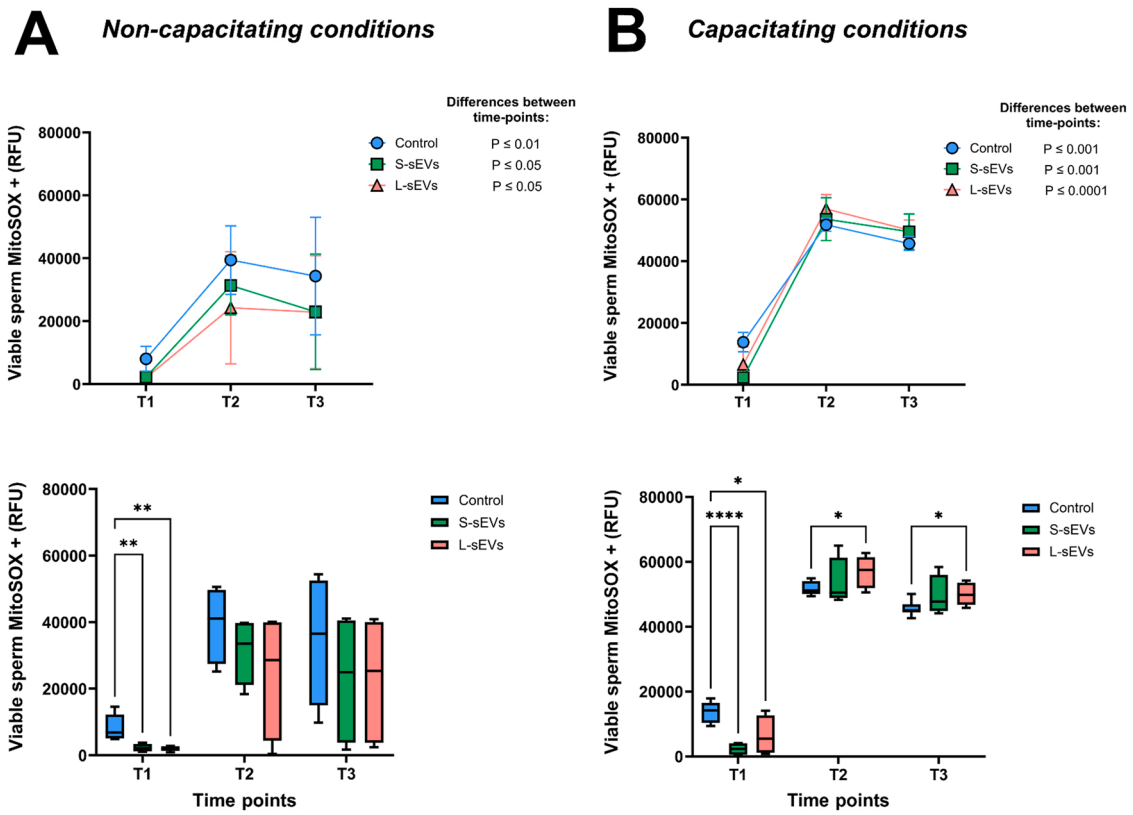

Fig. 5. Viable sperm with mitochondrial $O_2^{\bullet-}$ production (measured as Relative Fluorescence Units [RFU]) in porcine liquid-stored sperm samples incubated with small (S-, green), large (L-, red), or no (control, blue) seminal extracellular vesicles (sEVs) under (**A**) non-capacitating and (**B**) capacitating conditions. Data are shown at three different time-points of incubation at 37 ºC, 5 % CO_2 and 100 % humidity: 30 min (T1), 3 h (T2), and 6 h (T3). The upper graphs show the mean ± SEM, and the lower graphs show box plots (boxes enclose the 25th and 75th percentiles, whiskers extend to the 5th and 95th percentiles, and the line represents the median). Four biological replicates were performed. Differences between time points within each treatment are indicated on the right side of the upper graphs. Differences between treatments are shown in the lower graphs. * $P \leq 0.05$, ** $P \leq 0.01$, **** $P \leq 0.0001$, and n.s.: no significant.

interaction under the three evaluated pH conditions, the subsequent functional experiment was conducted at pH 7.0. This is also the most common pH of commercial liquid-stored seminal AI doses used in the pig industry (Gadea, 2003).

The role of sEVs in sperm function remains controversial (Roca et al., 2022). Discrepancies among studies may be due to the heterogeneity in experimental conditions or the presence of different sEV subsets in the raw sEV population. Accordingly, this study evaluated the effect of two phenotypically and compositionally different sEV subsets (Barranco et al., 2024a, 2023) on specific and relevant sperm functions. Interestingly, both sEV subsets had a similar effect on the evaluated sperm functionality parameters suggesting that, despite their molecular composition differences (Barranco et al., 2023), both sEV subsets contain a wide variety of molecular components involved in modulating sperm functions.

One of the most interesting findings of this study was that both sEV subsets decreased total ROS production in sperm. Although physiological levels of ROS are required for key sperm functions, such as capacitation (De Lamirande et al., 1997), excessive levels that surpass the capacity of the sperm antioxidant system led to oxidative stress (OS). OS causes lipid peroxidation of the sperm plasma membrane and DNA damage, which ultimately impairs the ability of sperm to fertilize and contributes to male infertility (Bansal and Bilaspuri, 2011; Guthrie and Welch, 2012). The present results indicated that sEVs would have a protective effect against OS by reducing ROS levels. These findings align with previous research showing that sEVs decrease ROS levels in human (Mahdavinezhad et al., 2022; Wang et al., 2022) and bovine sperm (Pal et al., 2025). Notably, Mahdavinezhad et al., (2022) observed reduced ROS generation in frozen-thawed sperm treated with exosomes and microvesicles. This demonstrates that both small (exosomes) and large (microvesicles or ectosomes) sEVs can modulate OS in sperm. Similarly, increased antioxidant activity has been observed in porcine and human sperm samples exposed to sEVs (Du et al., 2016; Mahdavinezhad et al., 2022; Wang et al., 2022). Proteomic analyses have identified key antioxidant enzymes, including ROS scavengers such as glutathione transferases and peroxidases, in sEVs (Taylor et al., 2013; Wang et al., 2022; Zhang et al., 2020). Antioxidant enzymes have also been found in porcine sEVs (Barranco et al., 2023). These sEVs would transfer these ROS scavengers to sperm (Chiaradia et al., 2021). Interestingly, the decrease in total ROS was accompanied by a decrease in mitochondrial $O_2^{\bullet-}$ production. This finding is consistent with that of Pal et al., (2025), who also reported a decreased mitochondrial $O_2^{\bullet-}$ production in bovine sperm exposed to sEVs. Therefore, it is plausible that sEVs transfer these ROS scavengers to

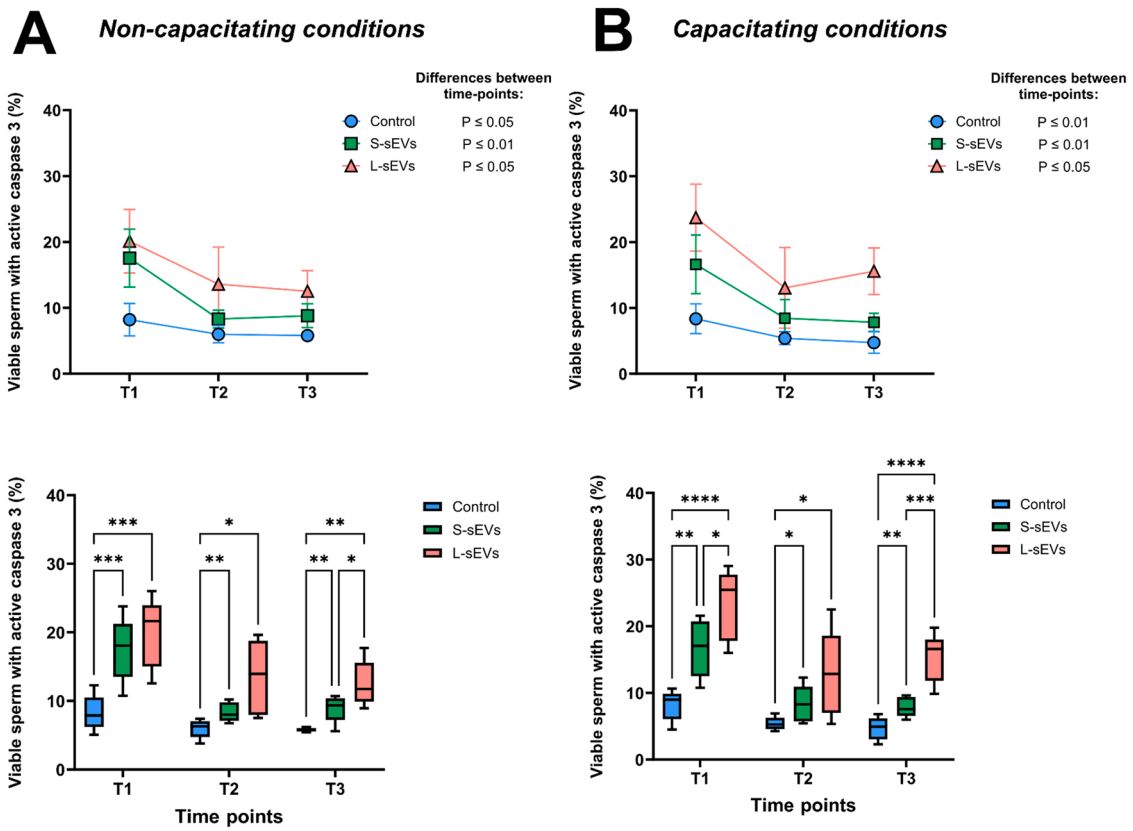

Fig. 6. Percentage of viable sperm undergoing apoptosis (active caspase-3) in porcine liquid-stored sperm samples incubated with small (S-, green), large (L-, red) or no (control, blue) seminal extracellular vesicles (sEVs) under (**A**) non-capacitating and (**B**) capacitating conditions. Data are shown at three different time points of incubation at 37 ºC, 5 % CO_2 and 100 % humidity: 30 min (T1), 3 h (T2), and 6 h (T3). The upper graphs show the mean ± SEM, and the lower graphs show box plots (boxes enclose the 25th and 75th percentiles, whiskers extend to the 5th and 95th percentiles, and the line represents the median). Four biological replicates were performed. Differences among time points within each treatment are indicated on the right side of the upper graphs. Differences among treatments are shown in the lower graphs. * $P \leq 0.05$, ** $P \leq 0.01$, *** $P \leq 0.001$, **** $P \leq 0.0001$, and ns: not significant.

spermatozoa, promoting the conversion of mitochondrial $O_2^{\bullet -}$ to H_2O_2 *via* superoxide dismutase (SOD), which then converts the H_2O_2 to H_2O *via* glutathione peroxidase. This hypothesis is supported by the results of Kowalczyk and Kordan, (2024), who found higher SOD levels frozen-thawed bull sperm exposed to sEVs. Ribas-Maynou et al., (2025) demonstrated that porcine sEVs protect DNA from OS, which also supports the above hypothesis.

Our results also showed that the two sEV subsets decreased MMP of sperm. MMP assessment is commonly used as a marker of mitochondrial function in sperm because it reflects the ability of mitochondria to generate ATP through oxidative phosphorylation (Shao et al., 2018). ATP is necessary for many sperm functions, including motility, hyperactivation, capacitation, and the acrosome reaction (Durairajanayagam et al., 2021). A reduction in MMP could indicate a decrease in mitochondrial activity, including ATP synthesis. This finding is supported by the results of our previous study, which demonstrated that sEVs reduced the ATP production in frozen-thawed pig sperm *via* mitochondrial oxidative phosphorylation (Barranco et al., 2024b). Additionally, the positive relationship between MMP and ROS production (Zorova et al., 2018), suggested that the decrease in total ROS levels observed in our sperm samples incubated with sEVs may be partially due to reduced mitochondrial activity. However, Mahdavinezhad et al., (2022) and Kowalczyk and Kordan, (2024) reported an increase in MMP in human and bull sperm exposed to sEVs prior to cryopreservation. These conflicting results may be due to species-specific differences or variations in experimental conditions (liquid storage *vs* cryopreservation) or assessment procedures (tetramethylrhodamine *vs* JC-1 [5,5',6,6'-tetrachloro-1,1',3,3'-tetraethyl- benzimidazolylcarbocyanine chloride]).

Interestingly, both sEV subsets increased caspase-3 activity in spermatozoa. Caspase-3, a protease, plays a pivotal role in the apoptotic pathway of sperm (Zhang et al., 2013) by controlling DNA damage and morphologic changes associated with apoptosis (Lakhani et al., 2006). The increase in caspase-3 activity suggests that sEVs may trigger or modulate apoptotic pathways, independently of capacitation stimuli. Notably, porcine sEVs contain caspase-3 (Barranco et al., 2023), which can be transferred to sperm and contribute to the observed effects. However, these findings contrast with those of Mahdavinezhad et al., (2022), who reported that exposure of human sperm to sEVs did not affect apoptosis levels, measured with Annexin V, in cryopreserved sperm. In this regard,

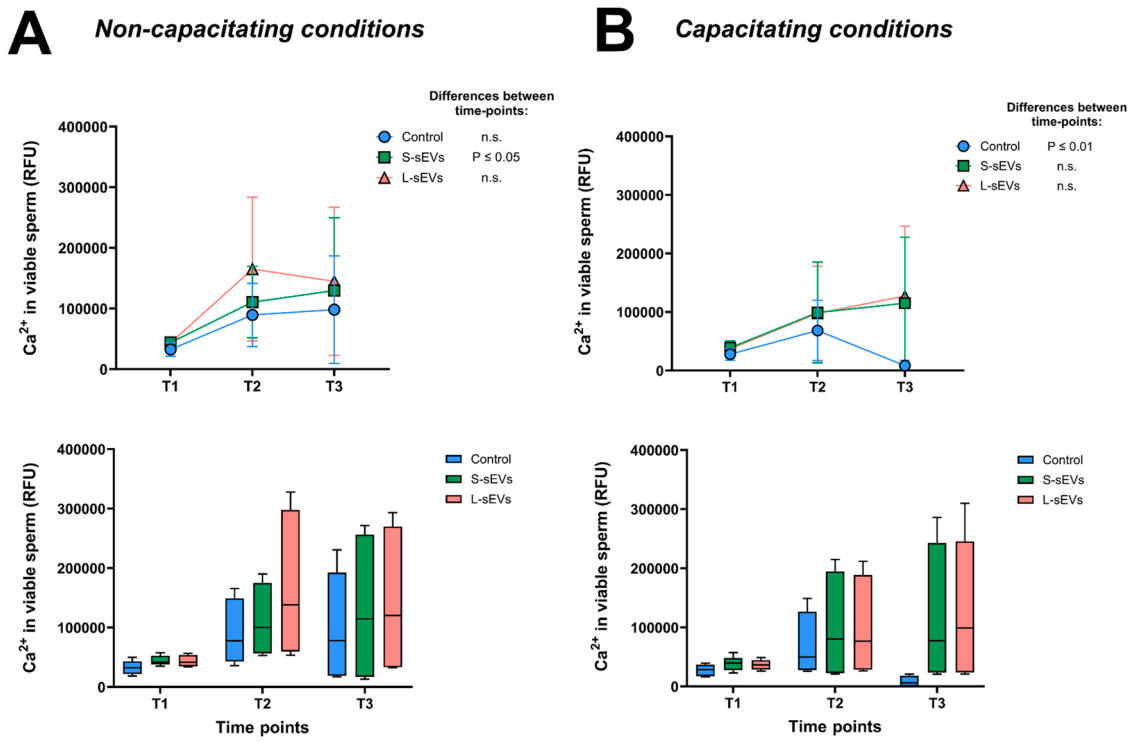

Fig. 7. Viable sperm with intracellular Ca^{+2} (estimated as Relative Fluorescence Units [RFU]) in porcine liquid-stored sperm samples incubated with small (S-, green), large (L-, red), or no (control, blue) seminal extracellular vesicles (sEVs) under (**A**) non-capacitating and (**B**) capacitating conditions. Data are shown at three different time points of incubation at 37 ºC, 5 % CO_2 and 100 % humidity: 30 min (T1), 3 h (T2), and 6 h (T3). The upper graphs show the mean ± SEM, and the lower graphs show box plots (boxes enclose the 25th and 75th percentiles, whiskers extend to the 5th and 95th percentiles, and the line represents the median). Four biological replicates were performed. Differences between time points within each treatment are indicated on the right side of the upper graphs. n.s.: no significant.

Ding et al., (2021) showed that sEVs transfer microRNA-222 to sperm. This microRNA inhibits pro-apoptotic genes, including CASP3. These discrepancies may be associated with differences in experimental conditions across studies and highlight the complex and context-dependent role of sEVs in sperm physiology.

The role of sEVs in modulating sperm capacitation is controversial. Some studies reported inhibitory effects (Bechoua et al., 2011; Pal et al., 2025; Piehl et al., 2013; Pons-Rejraji et al., 2011), while others have report stimulatory effects (Murdica et al., 2019; Wang et al., 2022), or even no effects (Aalberts et al., 2013; Barranco et al., 2024b; Tamessar et al., 2024). These inconsistencies may be attributed to several factors, such as the sEV-to-sperm ratio (Du et al., 2016; Pons-Rejraji et al., 2011), the SP source used to isolate the sEVs (Murdica et al., 2019), or other factors. Most of these studies have assessed sperm capacitation *via* analysis of tyrosine phosphorylation. In a previous study, however, we did not observe any effect of sEVs on sperm tyrosine phosphorylation (Barranco et al., 2024b). Therefore, we assessed sperm capacitation by analyzing intracellular Ca^{2+} levels because the influx of Ca^{2+} represents one of the earliest and more critical events of sperm capacitation (Breitbart, 2002). Our results showed that sEVs did not modify sperm intracellular Ca^{2+} levels. This indicates that sEVs may not be involved in regulating this early capacitation-related event in porcine spermatozoa. However, Palmerini et al., (1999) reported an increase of intracellular Ca^{2+} levels in human spermatozoa exposed to sEVs. These contradictory results could be due to species-specific differences, though they could also be due to differences in experimental designs or to the procedure used to isolate EVs. There are clear differences in the morphological integrity and purity of the EVs isolated by different procedures, and SEC is considered one of the most effective (Monguió-Tortajada et al., 2019).

The role of sEVs in modulating the acrosome reaction is still under debate (Roca et al., 2022). Some studies have reported that sEVs promotes it (Palmerini et al., 2003; Siciliano et al., 2008), while others have found an inhibitory effect (Pons-Rejraji et al., 2011; Xu et al., 2024) or no effect (Barranco et al., 2024b; Piehl et al., 2013; Rowlison et al., 2021; Tamessar et al., 2024). In our study, we found that sEVs influence the acrosome reaction in a time- and context-dependent manner. Specifically, we detected an early and transient increase in the percentage of acrosome-reacted sperm after 30-min incubation under non-capacitating conditions. This may potentially be mediated by bioactive molecules carried by sEVs that promote membrane destabilization. Porcine sEVs are enriched in proteins involved in acrosome exocytosis (Barranco et al., 2023), such as SNARE proteins or Rab GTPases (Kierszenbaum, 2000; Tomes et al., 2002). These proteins could be transferred from sEVs to sperm to promote acrosome reaction. Surprisingly, we observed an inhibition of the acrosome reaction after more prolonged sEV exposure time, which supports the notion that this process is modulated by sEVs in a time-dependent manner, as previously reported (Murdica et al., 2019; Pons-Rejraji et al., 2011). In addition to exposure duration, factors such as the sEV-to-sperm ratio and the composition of the incubation medium have been shown to modulate the impact of sEVs

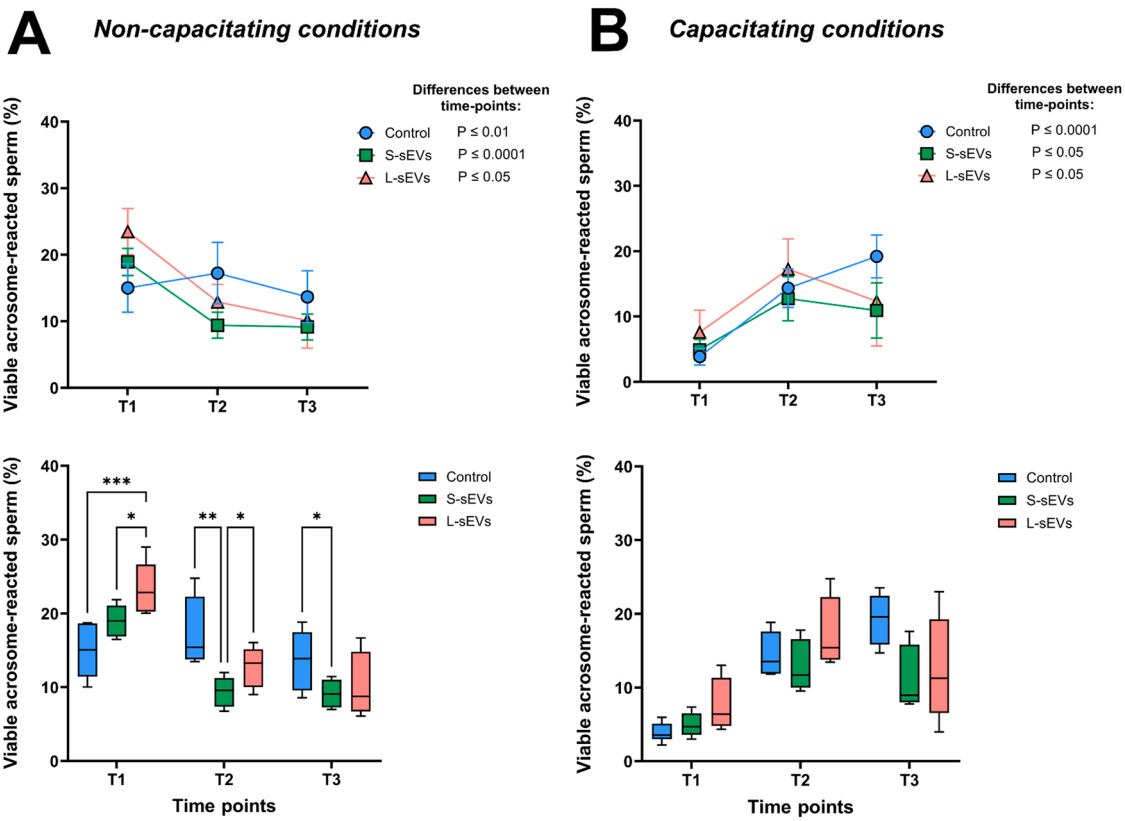

Fig. 8. Percentage of viable acrosome-reacted sperm in porcine liquid-stored sperm samples incubated with small (S-, green), large (L-, red), or no (control, blue) seminal extracellular vesicles (sEVs) under (**A**) non-capacitating and (**B**) capacitating conditions. Data are shown at three different time points of incubation at 37 ºC, 5 % CO_2 and 100 % humidity: 30 min (T1), 3 h (T2), and 6 h (T3). The upper graphs show the mean ± SEM, and the lower graphs show box plots (boxes enclose the 25th and 75th percentiles, whiskers extend to the 5th and 95th percentiles, and the line represents the median). Four biological replicates were performed. Differences among time points within each treatment are indicated on the right side of the upper graphs. Differences among treatments are shown in the lower graphs. * $P \leq 0.05$, ** $P \leq 0.01$, and *** $P \leq 0.001$.

on the acrosome reaction in porcine sperm (Du et al., 2016; Xu et al., 2024). Together, these findings underscore the complexity of sEV-mediated modulation of sperm function.

5. Conclusion

In conclusion, this study sheds new light on the interaction between sperm and two phenotypically and compositionally distinct sEV subsets. Both sEV subsets were able to bind to and fuse with liquid-stored porcine sperm across a wide range of pH conditions relevant to sperm physiology. These sEV subsets influenced sperm functionality similarly. They reduced total ROS and MMP and mitochondrial $O_2^{\bullet -}$ production, suggesting that they play a role in maintaining the sperm oxidative balance, probably by transferring antioxidant molecules to spermatozoa and/or modulating their mitochondrial activity. These sEV subsets would also influence sperm apoptotic pathways by increasing caspase-3 activity. Furthermore, they also modulate the acrosome reaction in a time- and context-dependent manner, inducing an early and transient increase in the number of viable acrosome-reacted sperm under non-capacitating conditions. Taken together, these results underscore the biological relevance of sEVs in pig sperm function.

CRediT authorship contribution statement

Patricia Panalés: Visualization, Methodology, Investigation. **Pablo Martínez-Díaz:** Visualization, Methodology, Investigation. **Martín-Cano Francisco Eduardo:** Validation, Investigation, Formal analysis, Data curation. **Ana Parra:** Writing – original draft, Visualization, Methodology, Investigation. **Isabel Barranco:** Writing – review & editing, Supervision, Resources, Funding acquisition, Formal analysis, Conceptualization. **Peña Fernando Juan:** Supervision, Resources, Formal analysis. **Jordi Roca:** Writing – review & editing, Validation, Supervision, Resources, Funding acquisition, Formal analysis, Conceptualization. **Xiomara Lucas:** Writing – review & editing, Supervision, Methodology, Investigation, Funding acquisition, Conceptualization.

Funding

The study was funded by the following grants: (1) PID2020–113493RB-I00 funded by (Ministry of Science, Innovation and Universities, Spain [MICIU]) MICIU/AEI/10.13039/501100011033; (2) PID2022–137738NA-I00 funded by MICIU/AEI/10.13039/501100011033 and ERDF/EU; (3) RYC2021–034546-I funded by MICIU/AEI/10.13039/501100011033 and European Union Next-GenerationEU/PRTR; and (4) 21935/PI/22 funded by Seneca Foundation (Murcia, Spain).

Declaration of Competing Interest

The authors declare that they have no conflicts of interest. The funders had no influence on the contents of the manuscript.

Acknowledgments

The authors thank AIM Ibérica (Topigs Norsvin Ibérica, Madrid, Spain) for providing the boar semen samples and the Service of Techniques Applied to Biosciences at the University of Extremadura (Spain) for their technical support.

Appendix A. Supporting information

Supplementary data associated with this article can be found in the online version at doi:10.1016/j.anireprosci.2025.108009.

References

Aalberts, M., Sostaric, E., Wubbolts, R., Wauben, M.W.M., Nolte-'T Hoen, E.N.M., Gadella, B.M., Stout, T.A.E., Stoorvogel, W., 2013. Spermatozoa recruit prostasomes in response to capacitation induction. Biochim. Biophys. Acta Proteins Prote 1834, 2326–2335. https://doi.org/10.1016/j.bbapap.2012.08.008.

Arienti, G., Carlini, E., Palmerini, C.A., 1997. Fusion of human sperm to prostasomes at acidic ph. J. Membr. Biol. 155, 89–94. https://doi.org/10.1007/S002329900160.

Bansal, A.K., Bilaspuri, G.S., 2011. Impacts of oxidative stress and antioxidants on semen functions. Vet. Med. Int. 2011, 686137. https://doi.org/10.4061/2011/686137.

Barranco, I., Sanchez-López, C.M., Bucci, D., Alvarez-Barrientos, A., Rodriguez-Martinez, H., Marcilla, A., Roca, J., 2023. The proteome of large or small extracellular vesicles in pig seminal plasma differs, defining sources and biological functions. Mol. Cell Proteom. 22, 100514. https://doi.org/10.1016/j.mcpro.2023.100514.

Barranco, I., Spinaci, M., Nesci, S., Mateo-Otero, Y., Baldassarro, V.A., Algieri, C., Bucci, D., Roca, J., 2024b. Seminal extracellular vesicles alter porcine in vitro fertilization outcome by modulating sperm metabolism. Theriogenology 219, 167–179. https://doi.org/10.1016/J.THERIOGENOLOGY.2024.02.024.

Barranco, I., Alvarez-Barrientos, A., Parra, A., Martínez-Díaz, P., Lucas, X., Roca, J., 2024a. Immunophenotype profile by flow cytometry reveals different subtypes of extracellular vesicles in porcine seminal plasma. Cell Commun. Signal 22, 63. https://doi.org/10.1186/S12964-024-01485-1.

Becerro-Rey, L., Martín-Cano, F.E., Fabres Robaina Sancler-Silva, Y., Gil, M.C., Ortega-Ferrusola, C., Aparicio, I.M., Gaitskell-Phillips, G., da Silva-Álvarez, E., Peña, F. J., 2024. In vitro, the aging of stallion spermatozoa at 22 °C is linked to alteration in Ca2+ and redox homeostasis and May be slowed by regulating metabolism. Theriogenology 229, 127–137. https://doi.org/10.1016/j.theriogenology.2024.08.021.

Bechoua, S., Rieu, I., Sion, B., Grizard, G., 2011. Prostasomes as potential modulators of tyrosine phosphorylation in human spermatozoa. Syst. Biol. Reprod. Med 57, 139–148. https://doi.org/10.3109/19396368.2010.549538.

Bordanaba-Florit, G., Royo, F., Kruglik, S.G., Falcón-Pérez, J.M., 2021. Using single-vesicle technologies to unravel the heterogeneity of extracellular vesicles. Nat. Protoc. 16, 3163–3185. https://doi.org/10.1038/S41596-021-00551-Z.

Breitbart, H., 2002. Role and regulation of intracellular calcium in acrosomal exocytosis. J. Reprod. Immunol. 53, 151–159. https://doi.org/10.1016/S0165-0378(01)00085-7.

Chiaradia, E., Tancini, B., Emiliani, C., Delo, F., Pellegrino, R.M., Tognoloni, A., Urbanelli, L., Buratta, S., 2021. Extracellular vesicles under oxidative stress conditions: biological properties and physiological roles. Cells 10, 1763. https://doi.org/10.3390/CELLS10071763.

Colombo, M., Raposo, G., Théry, C., 2014. Biogenesis, secretion, and intercellular interactions of exosomes and other extracellular vesicles. Annu Rev. Cell Dev. Biol. 30, 255–289. https://doi.org/10.1146/annurev-cellbio-101512-122326.

Cordeiro, L., Lin, H.L.H., Carvalho, A.V., Grasseau, I., Uzbekov, R., Blesbois, E., 2021. First insights on seminal extracellular vesicles in chickens of contrasted fertility. Reproduction 161, 489–498. https://doi.org/10.1530/REP-20-0462.

De Lamirande, E., Jiang, H., Zini, A., Kodama, H., Gagnon, C., 1997. Reactive oxygen species and sperm physiology. Rev. Reprod. 2, 48–54. https://doi.org/10.1530/ROR.0.0020048.

Ding, Y., Ding, N., Zhang, Y., Xie, S., Huang, M., Ding, X., Dong, W., Zhang, Q., Jiang, L., 2021. MicroRNA-222 transferred from semen extracellular vesicles inhibits sperm apoptosis by targeting BCL2L11. Front Cell Dev. Biol. 9, 736864. https://doi.org/10.3389/FCELL.2021.736864.

Doyle, L.M., Wang, M.Z., 2019. Overview of extracellular vesicles, their origin, composition, purpose, and methods for exosome isolation and analysis. Cells 8, 727. https://doi.org/10.3390/cells8070727.

Du, J., Shen, J., Wang, Y., Pan, C., Pang, W., Diao, H., Dong, W., 2016. Boar seminal plasma exosomes maintain sperm function by infiltrating into the sperm membrane. Oncotarget 7, 58832–58847. https://doi.org/10.18632/ONCOTARGET.11315.

Durairajanayagam, D., Singh, D., Agarwal, A., Henkel, R., 2021. Causes and consequences of sperm mitochondrial dysfunction. Andrologia 53, e13666. https://doi.org/10.1111/AND.13666.

Gadea, J., 2003. Review: semen extenders used in the artificial inseminarion of swine. Span. J. Agric. Res. 1, 17–27. https://doi.org/10.5424/SJAR/2003012-17.

Guthrie, H.D., Welch, G.R., 2012. Effects of reactive oxygen species on sperm function. Theriogenology 78, 1700–1708. https://doi.org/10.1016/J.THERIOGENOLOGY.2012.05.002.

Hawke, D.C., Watson, A.J., Betts, D.H., 2021. Extracellular vesicles, microRNA and the preimplantation embryo: non-invasive clues of embryo well-being. Reprod. Biomed. Online 42, 39–54. https://doi.org/10.1016/J.RBMO.2020.11.011.

Jeppesen, D.K., Zhang, Q., Franklin, J.L., Coffey, R.J., 2023. Extracellular vesicles and nanoparticles: emerging complexities. Trends Cell Biol. 33, 667–681. https://doi.org/10.1016/J.TCB.2023.01.002.

Juyena, N.S., Stelletta, C., 2012. Seminal plasma: an essential attribute to spermatozoa. J. Androl. 33, 536–551. https://doi.org/10.2164/JANDROL.110.012583.

Kalluri, R., LeBleu, V.S., 2020. The biology, function, and biomedical applications of exosomes. Science 367, eaau6977. https://doi.org/10.1126/SCIENCE.AAU6977.

Kierszenbaum, A.L., 2000. Fusion of membranes during the acrosome reaction: a tale of two SNAREs. Mol. Reprod. Dev. 57, 309–310. https://doi.org/10.1002/1098-2795(200012)57:4.

Kowalczyk, A., Kordan, W., 2024. Evaluation of the effectiveness of the use of exosomes in the regulation of the mitochondrial membrane potential of frozen/thawed spermatozoa. PLoS One 19. https://doi.org/10.1371/JOURNAL.PONE.0303479.
Lakhani, S.A., Masud, A., Kuida, K., Porter, G.A., Booth, C.J., Mehal, W.Z., Inayat, I., Flavell, R.A., 2006. Caspases 3 and 7: key mediators of mitochondrial events of apoptosis. Science 311, 847–851. https://doi.org/10.1126/SCIENCE.1115035.
Lange-Consiglio, A., Capra, E., Monferini, N., Canesi, S., Bosi, G., Cretich, M., Frigerio, R., Galbiati, V., Bertuzzo, F., Cobalchini, F., Cremonesi, F., Gasparrini, B., 2022. Extracellular vesicles from seminal plasma to improve fertilizing capacity of bulls. Reprod. Fertil. 3, 313–327. https://doi.org/10.1530/RAF-22-0037.
Lee, J.A., Spidlen, J., Boyce, K., Cai, J., Crosbie, N., Dalphin, M., et al., 2008. MIFlowCyt: the minimum information about a flow cytometry experiment. Cytom. A 73, 926–930. https://doi.org/10.1002/CYTO.A.20623.
Machtinger, R., Baccarelli, A.A., Wu, H., 2021. Extracellular vesicles and female reproduction. J. Assist Reprod. Genet 38, 549–557. https://doi.org/10.1007/S10815-020-02048-2.
Mahdavinezhad, F., Gilani, M.A.S., Gharaei, R., Ashrafnezhad, Z., Valipour, J., Nashtaei, M.S., Amidi, F., 2022. Protective roles of seminal plasma exosomes and microvesicles during human sperm cryopreservation. Reprod. Biomed. Online 45, 341–353. https://doi.org/10.1016/j.rbmo.2022.03.033.
Martínez-Díaz, P., Parra, A., Sanchez-López, C.M., Marcilla, A., Bucci, D., Roca, J., Barranco, I., 2025. A Size-Exclusion Chromatography-Based procedure for isolating extracellular vesicle subsets from porcine seminal plasma. Methods Mol. Biol. 2897, 601–609. https://doi.org/10.1007/978-1-0716-4406-5_40.
Mishra, A., Ashary, N., Sharma, R., Modi, D., 2021. Extracellular vesicles in embryo implantation and disorders of the endometrium. Am. J. Reprod. Immunol. 85, e13360. https://doi.org/10.1111/AJI.13360.
Monguió-Tortajada, M., Gálvez-Montón, C., Bayes-Genis, A., Roura, S., Borràs, F.E., 2019. Extracellular vesicle isolation methods: rising impact of size-exclusion chromatography. Cell Mol. Life Sci. 76, 2369–2382. https://doi.org/10.1007/s00018-019-03071-y.
Murdica, V., Giacomini, E., Alteri, A., Bartolacci, A., Cermisoni, G.C., Zarovni, N., Papaleo, E., Montorsi, F., Salonia, A., Viganò, P., Vago, R., 2019. Seminal plasma of men with severe asthenozoospermia contain exosomes that affect spermatozoa motility and capacitation. Fertil. Steril. 111, 897–908.e2. https://doi.org/10.1016/j.fertnstert.2019.01.030.
Nakase, I., Ueno, N., Matsuzawa, M., Noguchi, K., Hirano, M., Omura, M., Takenaka, T., Sugiyama, A., Bailey Kobayashi, N., Hashimoto, T., Takatani-Nakase, T., Yuba, E., Fujii, I., Futaki, S., Yoshida, T., 2021. Environmental ph stress influences cellular secretion and uptake of extracellular vesicles. FEBS Open Bio 11, 753–767. https://doi.org/10.1002/2211-5463.13107.
Pal, A., Karanwal, S., Habib, M.A., Josan, F., Gaur, V., Patel, A., Garg, M., Bhakat, M., Datta, T.K., Kumar, R., 2025. Extracellular vesicles in seminal plasma of sahiwal cattle bulls carry a differential abundance of sperm fertility-associated proteins for augmenting the functional quality of low-fertile bull spermatozoa. Sc. Rep. 15, 1–13. https://doi.org/10.1038/s41598-025-87998-2.
Palmerini, C.A., Carlini, E., Nicolucci, A., Arienti, G., 1999. Increase of human spermatozoa intracellular Ca2+concentration after fusion with prostasomes. Cell Calcium 25, 291–296. https://doi.org/10.1054/CECA.1999.0031.
Palmerini, C.A., Saccardi, C., Carlini, E., Fabiani, R., Arienti, G., 2003. Fusion of prostasomes to human spermatozoa stimulates the acrosome reaction. Fertil. Steril. 80, 1181–1184. https://doi.org/10.1016/S0015-0282(03)02160-5.
Park, K.H., Kim, B.J., Kang, J., Nam, T.S., Lim, J.M., Kim, H.T., Park, J.K., Kim, Y.G., Chae, S.W., Kim, U.H., 2011. Ca2+ signaling tools acquired from prostasomes are required for progesterone-induced sperm motility. Sci. Signal 4. https://doi.org/10.1126/scisignal.2001595.
Parolini, I., Federici, C., Raggi, C., Lugini, L., Palleschi, S., De Milito, A., Coscia, C., Iessi, E., Logozzi, M., Molinari, A., Colone, M., Tatti, M., Sargiacomo, M., Fais, S., 2009. Microenvironmental ph is a key factor for exosome traffic in tumor cells. J. Biol. Chem. 284, 34211–34222. https://doi.org/10.1074/JBC.M109.041152.
Phillips, W., Willms, E., Hill, A.F., 2021. Understanding extracellular vesicle and nanoparticle heterogeneity: novel methods and considerations. Proteomics 21, e2000118. https://doi.org/10.1002/PMIC.202000118.
Piehl, L.L., Fischman, M.L., Hellman, U., Cisale, H., Miranda, P.V., 2013. Boar seminal plasma exosomes: effect on sperm function and protein identification by sequencing. Theriogenology 79, 1071–1082. https://doi.org/10.1016/J.THERIOGENOLOGY.2013.01.028.
Pons-Rejraji, H., Artonne, C., Sion, B., Brugnon, F., Canis, M., Janny, L., Grizard, G., 2011. Prostasomes: inhibitors of capacitation and modulators of cellular signalling in human sperm. Int J. Androl. 34, 568–580. https://doi.org/10.1111/J.1365-2605.2010.01116.X.
Ribas-Maynou, J., Parra, A., Martínez-Díaz, P., Rubio, C.P., Lucas, X., Yeste, M., Roca, J., Barranco, I., 2025. Protective role of extracellular vesicles against oxidative DNA damage. Biol. Res. 58, 14. https://doi.org/10.1186/S40659-025-00595-5.
Roca, J., Rodriguez-Martinez, H., Padilla, L., Lucas, X., Barranco, I., 2022. Extracellular vesicles in seminal fluid and effects on Male reproduction. An overview in farm animals and pets. Anim. Reprod. Sci. 246, 106853. https://doi.org/10.1016/j.anireprosci.2021.106853.
Rodriguez-Martinez, H., Roca, J., 2022. Extracellular vesicles in seminal plasma: a safe and relevant tool to improve fertility in livestock? Anim. Reprod. Sci. 244, 107051. https://doi.org/10.1016/j.anireprosci.2022.107051.
Rodriguez-Martinez, H., Martinez, E.A., Calvete, J.J., Peña Vega, F.J., Roca, J., 2021. Seminal plasma: relevant for fertility? Int J. Mol. Sci. 22, 4368. https://doi.org/10.3390/ijms22094368.
Rodríguez-Martínez, H., Kvist, U., Ernerudh, J., Sanz, L., Calvete, J.J., 2011. Seminal plasma proteins: what role do they play? Am. J. Reprod. Immunol. 66 (1), 11–22. https://doi.org/10.1111/j.1600-0897.2011.01033.x.
Rowlison, T., Ottinger, M.A., Comizzoli, P., 2021. Exposure to epididymal extracellular vesicles enhances immature sperm function and sustains vitality of cryopreserved spermatozoa in the domestic cat model. J. Assist Reprod. Genet 38, 2061–2071. https://doi.org/10.1007/S10815-021-02214-0.
Schwarz, A., Wennemuth, G., Post, H., Brandenburger, T., Aumüller, G., Wilhelm, B., 2013. Vesicular transfer of membrane components to bovine epididymal spermatozoa. Cell Tissue Res. 353, 549–561. https://doi.org/10.1007/s00441-013-1633-7.
Shao, Y., Li, X., Wood, J.W., Ma, J. xing, 2018. Mitochondrial dysfunctions, endothelial progenitor cells and diabetic retinopathy. J. Diabetes Complicat. 32, 966–973. https://doi.org/10.1016/J.JDIACOMP.2018.06.015.
Siciliano, L., Marcianò, V., Carpino, A., 2008. Prostasome-like vesicles stimulate acrosome reaction of pig spermatozoa. Reprod. Biol. Endocrinol. 6, 5. https://doi.org/10.1186/1477-7827-6-5.
Tamessar, C., Trigg, N., Nixon, B., Skerrett-Byrne, D., Sharkey, D., Robertson, S., Bromfield, E., Schjenken, J., 2021. Roles of Male reproductive tract extracellular vesicles in reproduction. Am. J. Reprod. Immunol. 85, e13338. https://doi.org/10.1111/AJI.13338.
Tamessar, C.T., Anderson, A.L., Bromfield, E.G., Trigg, N.A., Parameswaran, S., Stanger, S.J., Weidenhofer, J., Zhang, H.-M., Robertson, S.A., Sharkey, D., Nixon, B., Schjenken, J.E., 2024. The efficacy and functional consequences of interactions between human spermatozoa and seminal fluid extracellular vesicles. Reprod. Fertil. 5, e230088. https://doi.org/10.1530/RAF-23-0088.
Taylor, A., Robson, A., Houghton, B.C., Jepson, C.A., Ford, W.C.L., Frayne, J., 2013. Epididymal specific, selenium-independent GPX5 protects cells from oxidative stress-induced lipid peroxidation and DNA mutation. Hum. Reprod. 28, 2332–2342. https://doi.org/10.1093/HUMREP/DET237.
Tomes, C.N., Michaut, M., Blas, G., De, Visconti, P., Matti, U., Mayorga, L.S., 2002. SNARE complex assembly is required for human sperm acrosome reaction. Dev. Biol. 243, 326–338. https://doi.org/10.1006/dbio.2002.0567.
Wang, H., Zhu, Y., Tang, C., Zhou, Z., Wang, Z., Li, Z., Zheng, X., Chen, S., Zhou, Y., Liang, A., Li, Y., Lin, Y., Sun, F., 2022. Reassessment of the proteomic composition and function of extracellular vesicles in the seminal plasma. Endocrinology 163, bqab214. https://doi.org/10.1210/endocr/bqab214.
Welsh, J.A., Goberdhan, D.C.I., O'Driscoll, L., Buzas, E.I., Blenkiron, C., Bussolati, B., et al., 2024. Minimal information for studies of extracellular vesicles (MISEV2023): from basic to advanced approaches. J. Extra Vesicles 13, e12404. https://doi.org/10.1002/JEV2.12404.
Xu, Zhiqian, Xie, Y., Wu, C., Gu, T., Zhang, X., Yang, J., Yang, H., Zheng, E., Huang, S., Xu, Zheng, Li, Z., Cai, G., Liu, D., Hong, L., Wu, Z., 2024. The effects of boar seminal plasma extracellular vesicles on sperm fertility. Theriogenology 213, 79–89. https://doi.org/10.1016/J.THERIOGENOLOGY.2023.09.026.

Zhang, J., Wang, X., Cui, W., Wang, W., Zhang, H., Liu, L., Zhang, Z., Li, Z., Ying, G., Zhang, N., Li, B., 2013. Visualization of caspase-3-like activity in cells using a genetically encoded fluorescent biosensor activated by protein cleavage. Nat. Commun. 4, 1–13. https://doi.org/10.1038/ncomms3157.
Zhang, X., Vos, H.R., Tao, W., Stoorvogel, W., 2020. Proteomic profiling of two distinct populations of extracellular vesicles isolated from human seminal plasma. Int J. Mol. Sci. 21, 7957. https://doi.org/10.3390/IJMS21217957.
Zorova, L.D., Popkov, V.A., Plotnikov, E.Y., Silachev, D.N., Pevzner, I.B., Jankauskas, S.S., Babenko, V.A., Zorov, S.D., Balakireva, A.V., Juhaszova, M., Sollott, S.J., Zorov, D.B., 2018. Mitochondrial membrane potential. Anal. Biochem. 552, 50–59. https://doi.org/10.1016/J.AB.2017.07.009.

Glossary

AI: Artificial insemination
EVs: Extracellular vesicles
fPBS: Filtered Phosphate buffered saline
L-sEVs: Large seminal extracellular vesicles
MIFlowCyt: Minimal Information About a Flow Cytometry Experiment
MISEV: Minimal information for studies of extracellular vesicles
MMP: Mitochondrial membrane potential
OS: Oxidative stress
PBS: Phosphate buffered saline
RFU: Relative fluorescence intensity
ROS: Reactive oxygen species
RT: Room temperature
SEC: Size exclusion chromatography
sEVs: Seminal extracellular vesicles
SOD: Superoxide dismutase
SP: Seminal plasma
S-sEVs: Small seminal extracellular vesicles